Solidification Behaviour of Mo$_x$TaNbVTi (x = 0,25 and 0,75) High Entropy Alloys

E Georgatis, A Poulia, C Mathiou, AE Karantzalis*

Dept. of Materials Science & Engineering, Univ. of Ioannina, Ioannina, Greece

Abstract

Mo$_x$TaNbVTi (x=0.25 at.% and 0.75 at.%) refractory high entropy alloys were successfully synthesized via vacuum arc melting. The work focuses on the evaluation of various parametric models for the formation of solid solution phases in the presented systems. The actual observation of the microstructures, along with the theoretical suggestions for solid solution formation was also discussed. Both systems experienced phase segregation phenomena, while an increase of the Mo content led to a significant grain refinement. Solidification parameter considerations and undercooling – recalescence issues were adopted, in order for the obtained grain refinement to be explained.

Keywords: High-Entropy Alloy; Microstructure; Electron Microscopy; Segregation; Refinement

Introduction

Lately, High Entropy Alloys (HEAs), a brand new category of advanced metallic materials, has dynamically been introduced into the metal materials field. This novel alloy design concept, has attracted worldwide attention and changed the past considerations. HEAs originally refer to multi-component (N≥5) solid solution phases, with equiatomic or near equiatomic concentrations between 5-35 at % [1]. The whole idea behind this innovative concept is based on the fact that compositional complexity may not necessarily lead to microstructural complexity (i.e. compound formation), due to the influence of entropy. More specifically, the preferred formation of solid solutions over intermetallic compounds originates from the high mixing entropy effect. Thermodynamically, a high entropy value significantly contributes to a decrease in the Gibbs energy of the solid solutions at elevated temperatures and hence wins the phase selection against intermetallic compounds [2-4]. During the last decade, several HEA systems based on transition elements have been synthesized, leading to a wide range of microstructures [5-9]. An intriguing combination of promising properties, such as exceptional specific strength, fracture toughness and superb mechanical properties, were also highlighted in most cases [10-15]. For example, light HEAs can easily be involved in the fields of transport and energy industry, where such leading materials are of great demand [16,17]. Towards this direction, new systems constantly appear in the scientific foreground, giving a boost to previously unexplored extensions. A characteristic example of such applications, targets on high melting point requirements. Among other materials, Refractory High Entropy Alloys (RHEAs) are also preferable in these cases, due to their promising outcomes [18-20]. For instance, during the last years of research activity on RHEAs, a huge variety of findings regarding their thermal stability and good oxidation performance has been recorded [21,22].

Meanwhile, both HEAs and RHEAs are ideally characterized by their single phase constitution, with face-centered cubic, body-centered cubic or hexagonal closely packed structures. The solid-state phase stability of HEAs originates from the thermodynamic balance between the limited enthalpy of formation and the high entropy of mixing, during the alloying procedure of equiatomic multicomponent elements [23]. Moreover, in many cases of HEA systems, a characteristic microstructure with dendritic features is observed [24-27]. Dendritic crystal growth within undercooled alloy melts is always accompanied by solute segregation, which drastically influences the structural morphology of the corresponding alloys [28]. A further experimental study on the characteristics of dendrite growth in multicomponent HEAs is highly desirable, as far as their undercooling and recalescensce are concerned. In the present work, the effort was focused on the examination of the microstructure of two Mo$_x$TaNbVTi refractory high entropy alloys with different Mo content and the correlation of their microstructural features with thermodynamic and solidification aspects.

Experimental Procedure

Mo$_x$TaNbVTi high entropy alloys (x= 0.25 and 0.75) were prepared by vacuum arc melting a mixture of their constituent elements with a purity over 99.5% in a water-cooled copper plate, under protective argon atmosphere. The raw materials were in the form of powders and/or wires. Repeated melting efforts were carried out at least five times to improve the homogeneous distribution of the elements in the final structure of the alloys. The examined systems provided appropriate data to study phase stability from the consideration of the fundamental properties of their constituent elements. Phase constitution was further analyzed by Scanning Electron Microscope (JEOL 6510 LV) equipped with both Backscatter Electron (BSE) and Energy Dispersive Spectroscopy (EDS) detectors (X-act, Oxford System).

Experimental Results and Discussion

Microstructural observations and parametric model criteria assessment

(Figure 1a, b) presents a panoramic view of the different materials microstructure produced in the present effort. It is clearly evident that, in both cases, phase segregation has taken place and all microstructures consist of two distinct phases: a light phase being the dominant phase and a dark phase mainly located at the interdendritic areas. Higher magnification of the received microstructures (Figure 2a, b) shows this segregation more intensively and EDS analysis of the involved phases indicates that the light phase is rich in Mo, Ta, Nb and V, whereas the dark phase is predominately consisted of Ti. Their actual composition is presented in (Table 1)

(Table 2), summarizes the predictions of the most commonly used, in the bibliography, parametric models for the different systems produced in the present effort, initially regarding their nominal targeted compositions. As data of (Table 2) reveal, a single phase solid solution is predicted for all different systems by all of the different models. More specifically, δ and ΔHmix values according to the model of Zhang et al [29] lay within their single phase stability range. Φ and δ values, as they proposed by King et al [30], are also within the proposed limits, suggesting the formation of a single phase solid solution. Troparevsky et al [31] model as well, shows that there is no tendency for the formation of an intermetallic phase and as such a single phase is also expected. In the case of Senkov et al [32] the k1cr factor is always higher than the ΔHmix/ΔHint ratio, which is the predominant condition for single phase formation. The first, however, suspicion about a possible phase segregation tendency arrives from the parametric model of Wang et al [33],
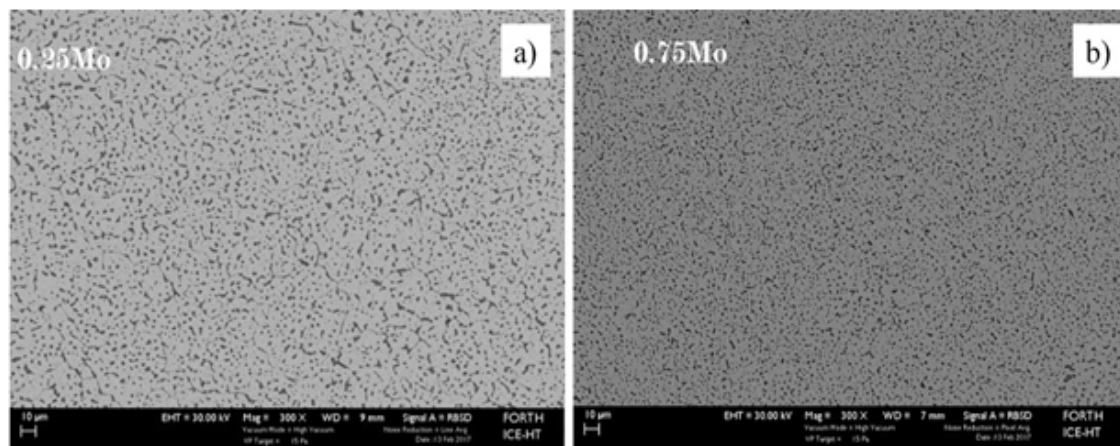

Figure 1: Panoramic view of the two different systems. Phase segregation and grain refinement are evident
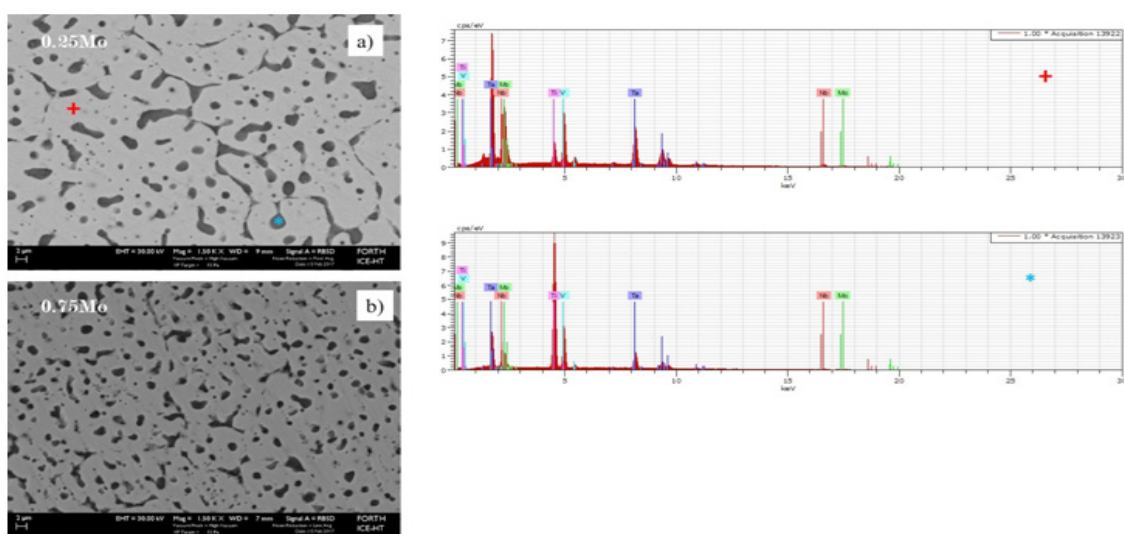

Figure 2: Higher magnification SEM images along with EDS analysis showing that the light phases is rich in all but Ti elements and the dark phase is rich in Ti

Citation: E Georgatis, A Poulia, C Mathiou, AE Karantzalis (2022) Solidification Behaviour of Mo$_x$TaNbVTi (x = 0,25 and 0,75) High Entropy Alloys. SOJ Mater Sci Eng 10(1): 1-10.

Page 2 of 10

Table 1: Actual compositions (at. %) of the observed phases in Mo0.25TaNbVTi and M0.75TaNbVTi alloys after EDS analysis

		Mo	Ta	Nb	V	Ti
0.25 Mo	at.% white (D)	2.66334	25.15459	23.86384	24.91845	13.39977
	at.% dark (ID)	0	3.024	4.072	5.882	87.024
0.75 Mo	at.% white (D)	20.19083	24.79831	22.37007	23.0095	9.631282
	at.% dark (ID)	0	2.294	3.156	5.148	89.408

Table 2: Parametric model predictions for different alloy nominal compositions

which is based on geometrical atomic radii considerations of the various involved elements. According to this model, the produced systems involve elements where the characteristic parameter γ is outside the limits for single phase formation. More specifically the model proposes values for γ below 1.175, whereas in the present case, the value of γ is 1.38. For further details of the adopted models, readers should address the relative bibliography. Despite the fact that the observed phase segregation was not predicted by most of the common parametric models, calculation based on the approach proposed by Senkov et al. in their early works [18], do support the phase segregation suspicion also arisen by Wang et al [33]. More specifically, Senkov et al [18], while dealing with MoTaNbVW equiatomic high entropy alloy, calculated the difference between the actual content of each element at the center of the primary phases and the average concentration of this element within the final alloy. They also correlated these differences with the difference of the element's melting point from the average melting point of the alloy, postulating that the higher the divergence from the straight line, the higher the tendency for segregation. (Figure 3a, b) represents this approach for the examined systems and as it can be seen in all cases, the involved elements tend to diverge from the straight line, a fact that could be another indication for phase segregation.

Furthermore, Senkov et al [18] calculated the distortion the 5th element will cause when it is to be accommodated within the lattice the other 4 elements have already formed. According to this approach, the higher the distortion, the more difficult the lattice to be stabilized and hence, the more intensive the tendency

for phase segregation is. Indeed, in the case of the here presented systems, as (Figure 4a, b) shows, V caused a severe lattice distortion when added to the other 4 element lattice, increasing in such way the difficulty for the 5 element lattice to be stabilized, enhancing, in turn, the possibility for phase segregation.

The actual microstructures and the previous conversation lead, thus, to the assumption that the parametric models did not succeed to predict the final phases. However, their validity should, by no means, be subjected into reconsideration. The primarily solidified phases (light phases) in all the different systems produced in the present effort; do fulfil the parametric model criteria. (Table 3), presents the predictions of three of the parametric models [29,30,33], where it can be observed that the calculated values, based on the actual compositions (Table 1), ley within the proposed single phase formation limits. Similar observations concerning the predictions of the stability of the primary phase by the parametric models can also be found in other research works [34-37].

As such, it should be noticed at this point that the parametric models can be a significantly useful tool in order to obtain valuable information on the behaviour of a potential new high entropy alloy system, especially at the initial designing stage. The final microstructure and involved phases, nevertheless, is by far a multi-parametric process, where more than thermodynamic, crystallographic, entropic and atomic size issues, such as solidification conditions and parameters, should be taken into consideration.
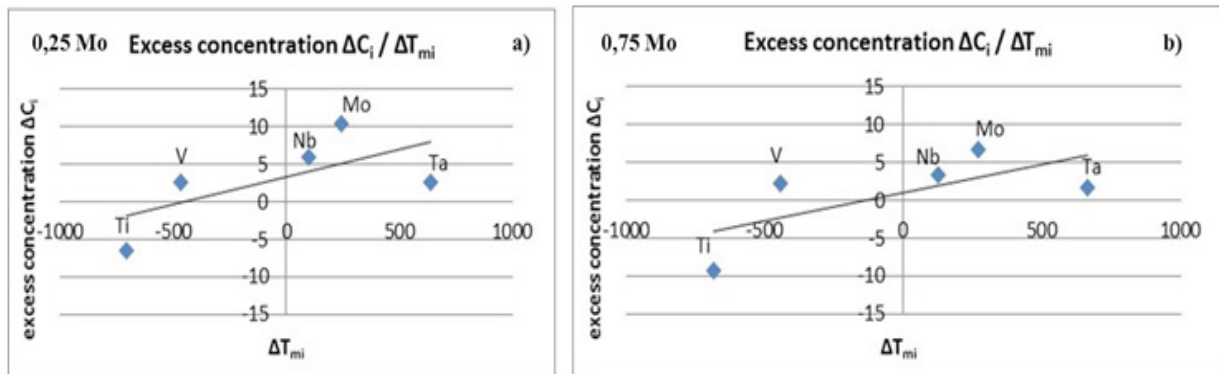
Citation: E Georgatis, A Poulia, C Mathiou, AE Karantzalis (2022) Solidification Behaviour of Mo$_x$TaNbVTi (x = 0,25 and 0,75) High Entropy Alloys. SOJ Mater Sci Eng 10(1): 1-10.

Page 3 of 10

Figure 3: Excess concentration of the ith element from the average value as a function the difference of its melting point from the average melting point of the system, according to postulates of Senkov et al.[18]. The higher the divergence from the straight line the higher the tendency for segregation
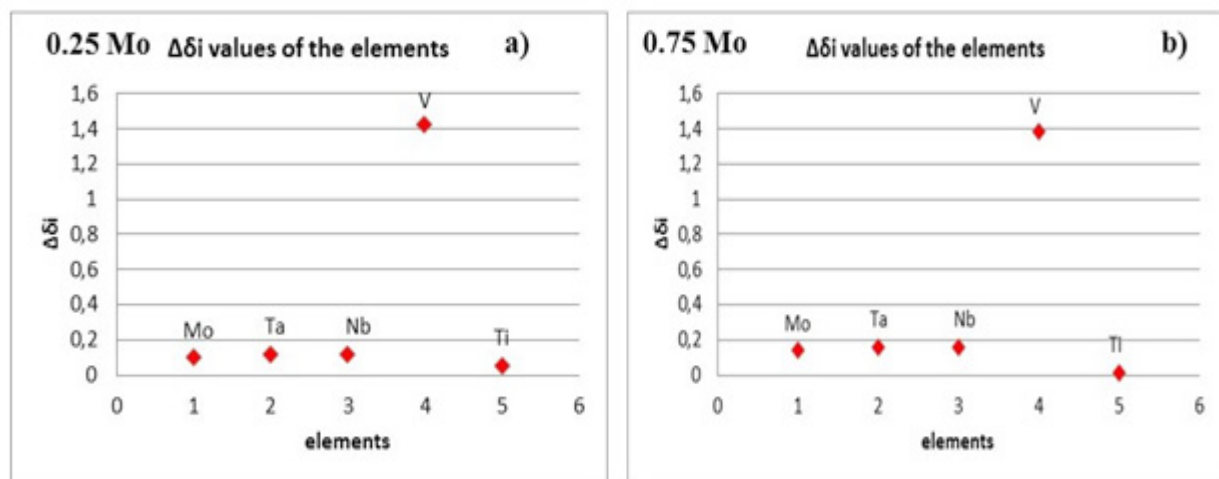

Figure 4: Distortion on the lattice of the quinary system by the addition of the 5th element. In both cases V destabilizes the lattice, by increasing the tendency for segregation

Based on the previous findings, an initial attempt to formulate a possible solidification sequence, should involve the following points, based on the data of (Tables 2-4) which include parametric model values for the elemental binary systems, related to the present case:

Ta, Mo, and Nb are the elements with the higher melting points. The ΔHmix values of binary MoTa, MoNb, MoV, TaNb, TaV, and NbV are negative, their Φ values are high and the distortion (δ) values are low, giving to Mo, Ta, Nb and V the potential to form solid solutions, without any preferential tendency for segregation in any of them.

The MoTi ΔHmix value is low negative but the NbTi, TaTi and VTi ΔHmix values are positive. Φ values for these pairs are approximately equal, except binary TaTi that gives almost double value. On the other hand δ value of NbTi is very low.

All these findings suggest that Ti is favorable to be partitioned in the dendrites and in the interdendritic region. As such, the

alloy is finally solidified with Mo, Ta, Nb, V and partly Ti in the dendrites and mainly Ti in the interdentritic region.

The effect of Mo content on grain refinement

One of the most important observations in the present effort, is the effect that Mo content has on the final microstructure. As shown in (Figures 1,2), an increase in Mo content leads to grain refinement of the microstructure. In order to explain this Mo effect, some fundamental solidification aspects should be recalled.

According to the solidification theory, grain refinement is a combination of two important factors: grain nucleation and growth. For a refinement of microstructure to be achieved, a high nucleation rate and a restricted grain growth are required [38,39]. Many factors can affect grain nucleation and growth, based on both intrinsic characteristics of the solidifying system (physicochemical and thermodynamic properties) and external parameters (casting processing, cooling rate and

Citation: E Georgatis, A Poulia, C Mathiou, AE Karantzalis (2022) Solidification Behaviour of Mo$_x$TaNbVTi (x = 0,25 and 0,75) High Entropy Alloys. SOJ Mater Sci Eng 10(1): 1-10.

Page 4 of 10

Table 3: Parametric model values for the primarily solidified phase in each alloy

	System	Proposed parametric models			
		δ	ΔH$_{mix}$	ΔS$_{mix}$	
Zhang [29]	0.25 Mo	3.7465	-8.43275	13.135	
	0.75 Mo	3.6806	-7.28004	13.113	
		Φ	δ	H$_{max}$	H$_{ss}$
King [30]	0.25 Mo	2.3999	3.64181	-14.889	-0.89987
	0.75 Mo	2.2459	3.60158	-16.685	-2.25467
		K$_1^{cr}$	ΔH$_{int}$	ΔH$_{int}$/ΔH$_{mix}$	
Senkov[32]	0.25 Mo	1.8259	-10.6246	1.26	
	0.75 Mo	1.9655	-12.9339	1.78	

other solidification conditions). Among these factors, however, undercooling and recalescensce seem to play a crucial role. Undercooling is the necessary temperature decrease below the liquids for nucleation to be initiated and recalescence is the following step of heat of fusion release. Schematically, for the readers' assistance, these two parameters are presented in (Figure 5). As far as the undercooling is concerned, it has been reported in the literature [40,43], that the degree of undercooling affects both the critical nuclei radius (r0) and the driving force for nucleation (ΔGnc):

$$r_0 = \frac{2\gamma_{SL}T_m}{L_V}\frac{1}{\Delta T}$$

$$\Delta G_{nc} = \frac{16\pi\gamma_{SL}^3 T_m^2}{3L_V^2}\frac{1}{\Delta T^2}$$

Where: γSL the solid-liquid interfacial energy, Tm the melting point, Lv the latent heat of fusion and ΔT the undercooling

It can be seen, thus, from the previous equations, that the higher the undercooling the more reduced the critical radius for nucleation, the lower the driving force for nucleation and the higher the nucleation rate [40,43], since both these factors are the main factors controlling the nucleation rate. It has also been reported that the higher the undercooling the higher the grain growth rate [28,40,41]. Both these outcomes support that the higher the cooling rate, the more intensive the microstructural grain refinement.

Recalescensce, on the other hand, can also significantly contribute to the microstructural refinement. According to the approaches [43,44]:

Low recalescence combined with liquid heat extraction lead to restriction of dendrite grain growth which practically means primary grain refinement

Medium recalescence combined with liquid heat extraction lead to an increase of dendrite trunk wall temperature and the development of a negative T gradient which in turns lead to the development of secondary dendrites

High degree of recalescensce may establish adiabatic conditions that may cause Raleigh – Taylor instabilities that can in turn cause dendrite fragmentation and eventually can lead to significant secondary grain refinement up to the level of grain bridging and grain boundary elimination.

Yang et al [43] and Karma [44] have also commented in their works on the interrelation between undercooling and recalescensce and concluded that a lower undercooling, despite the fact that results in lower temperature of the residual liquid, establishes a more prolonged duration of the recalescensce stage. It is proposed that a more prolonged recalescensce can lead to a more intensive grain refinement, due to more intensive dendrite fragmentation. Schematically, the postulates of Yang et al [43] and Karma [44] on the relation between recalescence and undercooling, are presented in (Figure 6).

All the statements of the previous paragraphs, will prove helpful to explain the refinement the different Mo content caused in the present effort. Before proceeding, however, it is very important to examine macroscopically, the different microstructures formed at different locations of a solidifying sample, so that to recognize the different cooling rates established in each area.

(Figure 7) shows a panoramic view of the cross section of MoTaNbVTi equi-atomic sample. It can be observed that there are areas of distinguishing different microstructures: a) An area close to the water cooled mold, where the microstructure is characteristically dendritic. This dendritic structure is gradually reduced towards the interior of the sample. b) An area at significant distance from the base, shows a microstructure where the dendritic characteristics are vanished, with the grains being almost equiaxed and practically coincided and bridged to each other.

In the first area, close to the copper base, it can be postulated that due to rapid heat extraction, recalescensce has limited time to express its effects and characteristics. The dendritic growth follows the heat extraction direction and large directional dendrites are formed, whereas moving away from the base, recalescensce is expressed more intensively, causing an increase
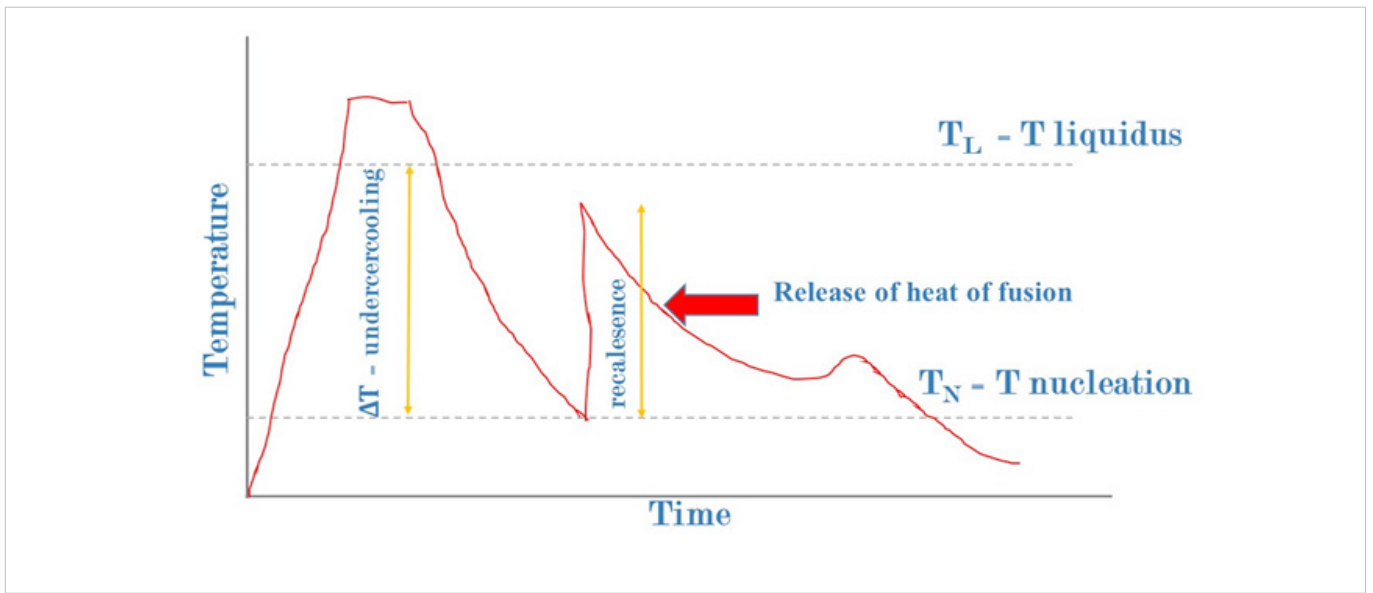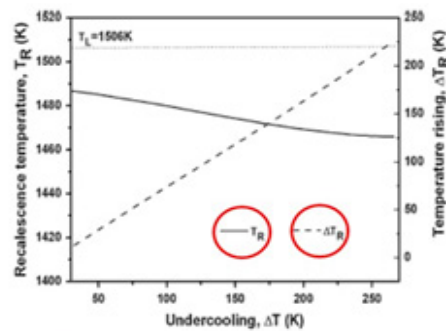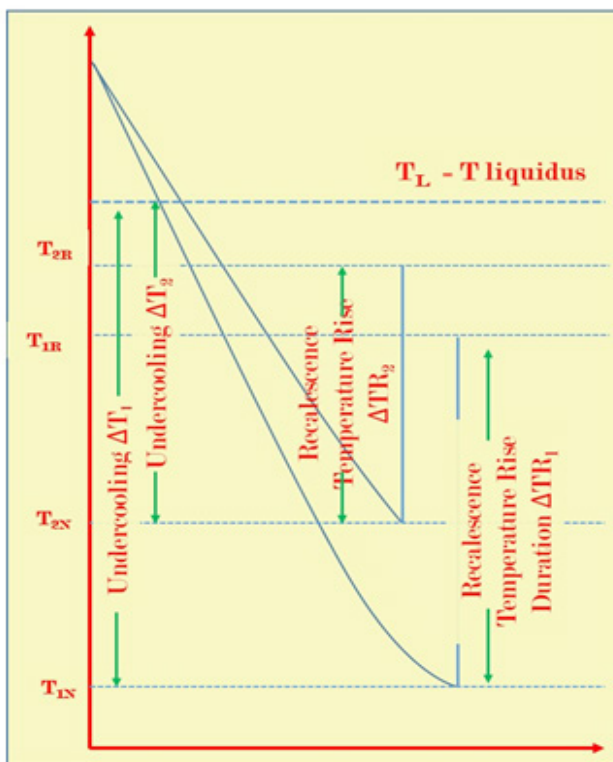
Citation: E Georgatis, A Poulia, C Mathiou, AE Karantzalis (2022) Solidification Behaviour of Mo$_x$TaNbVTi (x = 0,25 and 0,75) High Entropy Alloys. SOJ Mater Sci Eng 10(1): 1-10.

Page 5 of 10

Figure 5: Graphical representation of undercooling and recalescence

$$f_s = \frac{\Delta T_R C_p}{\Delta H} = \frac{(T_R + \Delta T - T_i)C_p}{\Delta H},$$

where: f$_s$ the fraction of the solid phase, ΔT the undercooling, ΔH the enthalpy of fusion, C$_p$ the heat capacity of the liquid, T$_R$ the recalescence maximum temperature of the melt, ΔT_R the temperature rise due to recalescence.

Figure 6: Schematic representation of Yang et al [43] approach. The higher the undercooling (ΔT) causes lower recalescence Temperature (TR) yet the duration of recalescence (ΔTR) is higher. This causes secondary grain refinement due to secondary arm fragmentation. In the case of high undercooling, adiabatic conditions are established leading to increase of the solid fraction (fs). This causes conjunction of grains by secondary grain bridging and, thus, to vagueness of the grain boundaries.

on the residual liquid temperature and restricting as such the dendritic growth leading to what is mentioned by Yang et al [43] as primary refinement. In areas considerably away from the base, quasi adiabatic conditions may be established and recalescensce may cause significant dendrite fragmentation and residual liquid fraction decrease. Both these two factors, according to Yang et al [43] can lead to secondary refinement, due to nucleation by the dendrite fragments along with grain bridging and conjunction. In the following paragraphs an attempt to correlate these speculations with the actual microstructures will be presented. The microstructures of the
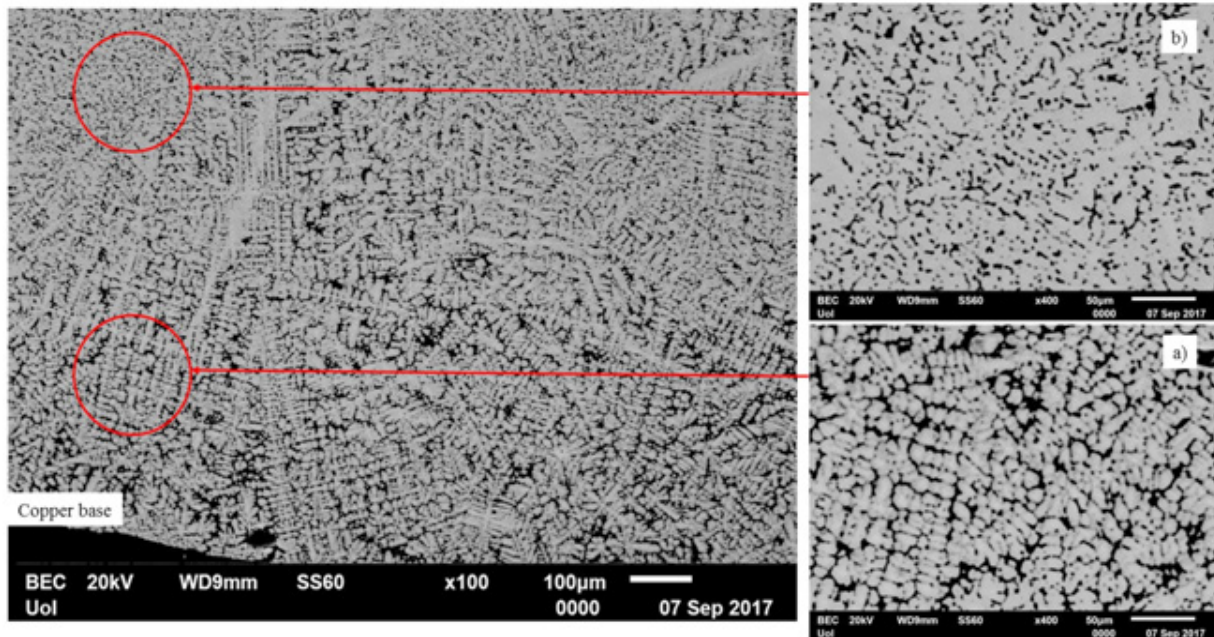
Citation: E Georgatis, A Poulia, C Mathiou, AE Karantzalis (2022) Solidification Behaviour of Mo$_x$TaNbVTi (x = 0,25 and 0,75) High Entropy Alloys. SOJ Mater Sci Eng 10(1): 1-10.

Page 6 of 10

Figure 7 a): Area close to the copper base: Rapid heat extraction i.e. limited time for recalesence to express its effects leading to dendritic growth following heat extraction. Directional mode fades moving away of the base, recalescene and heat release interrupts grain growth causing primary grain refinement. b) Area away from the base: Recalescence significantly developed causing dendrite fragmentation i.e. secondary grain refinement along with increased solid fraction and reduced residual liquid leading to refined grains bridging and eventually conjunction and fading of grain boundaries

0.25 Mo and 0.75 Mo are presented in (Figure 1). Both images have been received by similar areas, away from the copper base. The appearance of the their microstructure suggests, according to Yang's et al [43] thoughts, that the secondary grain refinement has taken place, due to recalescensce expression without, however, being so intensively to cause grain conjunction and grain boundary elimination. The question, though, why the 0.75 Mo microstructure is more refined has, yet, not been answered. The following analysis will attempt to clarify this phenomenon:

Effect of different cooling rate: Since both samples were received by almost the same distance of the copper base, it is reasonable to assume that cooling rate should not have any profound effect on the final microstructures. As such other factors should have played a predominant role.

Effect of different undercooling: The following points do support the fact that undercooling and recalescensce should play an important role.

Elemental partitioning: (Table 5) shows the distribution of the different elements between the dendritic and the interdendritic areas. A partition coefficient (K) is calculated for each element. The sum of these partitioning ratios (Ktotal) for each system shows that in the case of 0.75 Mo alloy the overall value is, although slight, still lower than in the case of 0.25 system. Lower partitioning suggests a smoother elemental distribution, which in turn can be associated with slower diffusion processes and slower solidification kinetics. In turn, slower solidification kinetics contribute to higher nucleation rates and retardation of growth, i.e to more intensive refinement. Similar observations have been documented by Senkov et al [18]

Liquidus suppression: Mo and Ta are the elements with the higher melting points and as such they lead the solidification process. According to the Mo –Ta phase diagram [45] the higher Mo content results in the lowering of the liquidus. Such suppression may cause a relative to the liquids increase of the residual liquid temperature, due to recalescensce and as such, a more intensive dendrite fragmentation and refinement. Suppression of liquidus also causes a narrowing of the solidification range, a fact that also results in a more intensive grain refinement process.

Grain growth retardation due to lattice distortion: (Table 6) shows the distortion the 5th element causes on the already formed quaternary system lattice. It can be seen that in the case of the 0.75 Mo alloy, at least for the three major elements of the primary phase (Mo, Ta and Nb), the lattice distortion these elements cause is higher than in the case of 0.25 Mo alloy. A higher degree of lattice distortion could be interpreted as an increased difficulty for the quaternary system to accommodate the 5th element. Such a difficulty can result in a retardation on the development of the lattice and as such of the growing grain. Growth restriction, as already mentioned, may cause more intensive grain refinement.

Different extent of recalescensce: Although recalescensce was not measured experimentally, there are strong indications that a higher recalescensce effect may have been expressed in the case of 0.75 Mo alloy. (Table 7) shows the calculated values of the basic parameters derived from the proposed models. It can be observed that the Hss value (the enthalpy of solid solution

Citation: E Georgatis, A Poulia, C Mathiou, AE Karantzalis (2022) Solidification Behaviour of Mo$_x$TaNbVTi (x = 0,25 and 0,75) High Entropy Alloys. SOJ Mater Sci Eng 10(1): 1-10.

Page 7 of 10

Table 4: Parametric model values for the binary systems involved in the present case. Calculations were conducted using the www.alloyASAP.com platform proposed by King et al[30].

Element pair	ΔHmix	δ	Φ	Element pair	ΔHmix	δ	Φ
MoTa	-193	2.4561	3.4139	NbV	-56	4.2857	7.4535
MoNb	-133	2.4561	2.9025	MoTi	-167	2.7972	3.6675
MoV	-127	1.8315	0	TaTi	31	0.3413	7.1283
TaNb	-10	0	0	NbTi	11	0.3413	3.7393
TaV	-122	4.2857	7.84004	VTi	37	4.6263	4.6447

Table 5: Elemental partitioning (K=CD/CID) for the two different systems and calculation of their total partition coefficient (Ktotal)

	0.25 Mo				
Average at. %	Mo	Ta	Nb	V	Ti
D	15.36	22.6	25.885	22.605	13.545
ID	5.195	7.745	9.695	9.15	62.215
K	2.956689	2.918012	2.669933	2.470492	0.198563
Ktotal	11.21				
	0.75 Mo				
Average at. %	Mo	Ta	Nb	V	Ti
D	21.8	21.745	23.445	22.27	10.74
ID	6.86	8.27	9.53	10.85	64.5
K	3.177843	2.629383	2.460126	2.052535	0.166512
Ktotal	10.48				

Table 6: Calculations of the lattice distortion caused by the 5th element, when to be accommodated within the lattice of the already formed quinary system for the two different systems examined

0.25 Mo	Mo	Ta	Nb	V	Ti
Δδi	0.09819	0.11819	0.119819	1.42181	0.05181
0.75 Mo	Mo	Ta	Nb	V	Ti
Δδi	0.13842	0.15842	0.15842	0.138158	0.01158

Table 7: Parametric model values for the primary phases of Mo0.25TaNbVTi and Mo0.75TaNbVTi HEAs according to King et al. model [30]. Notice the reduction in Hss values with increasing the Mo content

Alloy	Φ	δ	Hmax	Hss
0.25 Mo	2.399	3.64181	-14.899	-0.89987
0.75 Mo	2.2459	3.60158	-16.665	-2.25467

Table 8: Change in ΔHss values after the addition of the 5th element to the already formed quinary system. Notice the reduction in its values for every element with increasing the Mo content

0.25 Mo	Mo	Ta	Nb	V	Ti
Δ$_{ΔHss}$	-2.51987	0.087013	0.60013	1.83013	1.11013
0.75 Mo	Mo	Ta	Nb	V	Ti
Δ$_{ΔHss}$	-3.87467	-0.48467	-0.75467	0.47533	-0.244467

formation) is more negative in the case of 0.75 Mo system. Additionally, (Table 8) shows the change in the solid solution enthalpy of formation, ΔΔHss, caused by the incorporation of the 5th element in the already formed quaternary system, following the approach of Senkov et al [18] It can be observed, that in the case of 0.75 Mo alloy, these values are in general more negative than in the case of 0.25 Mo alloy. More negative Hss values and more negative ΔHss values suggest the release of higher amounts of heat of fusion after nucleation, i.e. a higher degree of recalescensce. As such, from the previous discussion, a more intensive grain refinement could be expected.

Citation: E Georgatis, A Poulia, C Mathiou, AE Karantzalis (2022) Solidification Behaviour of Mo$_x$TaNbVTi (x = 0,25 and 0,75) High Entropy Alloys. SOJ Mater Sci Eng 10(1): 1-10.

Page 8 of 10

Conclusion

In the present work Mo$_x$TaNbVTi (x=0.25 at.% and 0.75 at.%) refractory high entropy alloys were successfully prepared by vacuum arc melting processing. Both systems were experienced phase segregation phenomena, consisting of two major phases. Parametric model criteria, despite the fact that failed to predict the phase segregation, seem to be valid for the primarily solidified phase. An increase of Mo content led to a grain refinement of the final microstructure, while various solidification parameter considerations and undercooling – recalescensce issues were adopted in order for the obtained grain refinement to be explained.

References

1. Yeh JW, Chen SK, Lin SJ, Gan JY, Chin TS, Shun TT, et al. Nanostructured High-Entropy Alloys with Multiple Principal Elements: Novel Alloy Design Concepts and Outcomes. Adv Eng Mater. 2004;6:299-303

2. Yeh JW. Recent Progress in High Entropy Alloys. Ann Chim Sci Mater. 2006;31:633-648

3. Ranganathan. Alloyed Pleasures: Multimetallic Cocktails. Cur. Sci. 2003;85:1404-1406

4. Chun Ng, Sheng Guo, Junhua Luan, Sanqiang Shia, Liu. Entropy-Driven Phase Stability and Slow Diffusion Kinetics in Al0.5CoCrCuFeNi high entropy alloy. Intermetallics. 2012;31:165-172

5. Chung Tong, Liang Chen, Jien Yeh, Jien Lin, Kai Chen, Tsung Shun, Huei Tsau, Shou. Chang Microstructure Characterization of AlxCoCrCuFeNi High-Entropy Alloy System with Multiprincipal Elements. Metall Mater Trans A. 2005;36:881-893

6. Zhang, Ma SG, Qiao JW. Morphology Transition from Dendrites to Equiaxed Grains for AlCoCrFeNi High-Entropy Alloys by Copper Mold Casting and Bridgman Solidification. Metall Mater Trans A. 2012;43:2625-2630.

7. Wang X, Xie H, Jia L, Lu Z. Effect of Ti, Al and Cu Addition on Structural Evolution and Phase Constitution of FeCoNi System Equimolar Alloys. Mater Sci Forum. 2012;724:335-338

8. Praveen, Murty, Kottada RS. Alloying Behaviour in Multi-Component AlCoCrCuFe and NiCoCrCuFe High Entropy Alloys. Mater Sci Eng A, 2012;534:83-89

9. Liu L, Zhu JB, Zhang C, Li JC, Jiang Q. Microstructure and the Properties of FeCoCuNiSnx High Entropy Alloys. Mater Sci Eng A. 2012;548:64-68

10. Hemphill, Yuan, Wang, Yeh, Tsai, Chuang. Fatigue Behaviour of Al0.5CoCrCuFeNi High Entropy Alloys. Acta Mater. 2012;60:5723-5734.

11. Tariq, Naeem, Hasan, Akhter, Siddique. Effect of W and Zr on Structural, Thermal and Magnetic Properties of AlCoCrCuFeNi High Entropy Alloy. J Alloys Compd. 2013;556:79-85

12. Kuznetsov, Shaysultanov, Stepanov, Salishchev, Senkov. Tensile Properties of an AlCrCuNiFeCo High-Entropy Alloy in As-Cast and Wrought Conditions. Mater Sci Eng A. 2012;533:107-118

13. Zhuang, Liu, Chen, Xue. Effect of Elemental Interaction on Microstructure and Mechanical Properties of FeCoNiCuAl alloys. Mater Sci Eng A. 2012;556:395-399

14. Ye YF, Wang Q, Lu J, Liu CT, Yang Y. High-Entropy Alloy: Challenges and Prospects. Mater Today. 2016;19:349-362.

15. Zhang Y, Zuo TT, Tang Z, Gao MC, Dahmen, Liaw, et al. Microstructures and Properties of High-Entropy Alloys. Prog Mater Sci. 2014;61:1-93

16. Miracle, Miller, Senkov, Woodward, Uchic, Tiley. Exploration and Development of High Entropy Alloys for Structural Applications. Entropy. 2014;16:494-525

17. Yeh JW. Alloy Design Strategies and Future Trends in High-Entropy Alloys. JOM. 2013; 65:1759-1771

18. Senkov, Wilks, Miracle, Chuang, Liaw. Refractory High-Entropy alloys. Intermetallics. 2010;18:1758-1765

19. Senkov, Scott, Senkova, Meisenkothen, Miracle, Woodward. Microstructure and Elevated Temperature Properties of a Refractory TaNbHfZrTi Alloy. J Mater Sci. 2012;47:4062-4074

20. Gorr, Azim, Christ, Mueller, Schliephake, Heilmaier. Phase Equilibria, Microstructure, and High Temperature Oxidation Resistance of Novel Refractory High-Entropy Alloys. J Alloy Compd. 2015;624:270-278

21. Liu CM, Wang HM, Zhang SQ, Tang HB, Zhang AL. Microstructure and Oxidation Behaviour of New Refractory High Entropy Alloys. J Alloys Compd. 2014;583:162-169

22. Tsai MH, Wang CW, Tsai CW, Shen WJ, Yeh WJ, et al. Thermal Stability and Performance of NbSiTaTiZr High-Entropy Alloy Barrier for Copper Metallization. J Electrochen Soc. 2011;158:1161-1165

23. Tian FY, Delczeg L, Varga LK, Shen J, Vitos L. Structural Stability of NiCoFeCrAlx High-Entropy Alloy from Ab Initio Theory. Phys Rev B. 2013;88.

24. Senkov, Scotta, Senkova, Miracle, Woodward. Microstructure and Room Temperature Properties of a High-Entropy TaNbHfZrTi Alloy. J Alloys Compd. 2011;509:6043-6048

25. Couzinié, Dirras, Perrière, Chauveau, Leroy, Champion, et al. Microstructure of a Near-Equimolar Refractory High-Entropy Alloy. Mater Lett. 2014;126:285-287

26. Guo NN, Wang L, Luo LS, Li XZ, Chen. Microstructure and Mechanical Properties of In-Situ MC-Carbide Particulates-Reinforced Refractory High-Entropy Mo0.5NbHf0.5ZrTi Matrix Alloy Composite. Intermetallics. 2016;69:74-77

27. Wu YD, Cai YH, Chen XH, Wang T, Si JJ, Wang L, et al. Phase Composition and Solid Solution Strengthening Effect in TiZrNbMoV High-Entropy Alloys. Mater Des. 2015;83:651–660

28. Chang, Wan, Wei. Rapid Dendritic Growth Within an Undercooled Ni–Cu–Fe–Sn–Ge Quinary Alloy. Philos Mag Lett. 2008;88:821-828.

29. Zhang, Zhou, Lin, Chen, Liaw. Solid Solution Phase Formation Rules for Multi-Component Alloys. Adv Eng Mater. 2008;10:534-538

30. King, Middleburgh, McGregor, Cortie. Predicting the Formation and Stability of Single Phase High-Entropy Alloys. Acta Mater. 2016;104:172-179

31. Troparevsky, Morris, Kent, Lupini, Stocks. Criteria for Predicting the Formation of Single-Phase High-Entropy Alloys. Phys Rev X. 2015; 5:011041-1-011041-6

32. Senkov, Miracle. A New Thermodynamic Parameter to Predict Formation of Solid Solution or Intermetallic Phases in High Entropy Alloys. J Alloys Compd. 2016;658:603-607

33. Wang, Huang, Yang, Liu. Atomic-Size Effect and Solid Solubility of Multicomponent Alloys. Scripta Mater. 2015;94:28-31

34. Poulia, Georgatis, Mathiou, Karantzalis. Phase Segregation Discussion

Citation: E Georgatis, A Poulia, C Mathiou, AE Karantzalis (2022) Solidification Behaviour of Mo$_x$TaNbVTi (x = 0,25 and 0,75) High Entropy Alloys. SOJ Mater Sci Eng 10(1): 1-10.

Page 9 of 10

in a Hf25Zr30Ti20Nb15V10 High Entropy Alloy: The Effect of the High Melting Point Element. Mater. Chem Phys. 2017.

35. Mathiou, Poulia, Georgatis, Karantzalis. Microstructural Features and Dry Sliding Wear Response of MoTaNbZrTi High Entropy Alloy. Mater Chem Phys. 2018;210:126-135

36. Karantzalis, Poulia, Georgatis, Petroglou. Phase Formation Criteria Assessment on the Microstructure of a New Refractory High Entropy Alloy. Scripta Mater. 2017;131:51-54

37. Karantzalis, Poulia, Georgatis, Mathiou. New MoWHfZrTi High Entropy Alloy System: A Microstructural Verification of Phase Formation Criteria Approach. Res Rep Metals. 2017;1:1-6

38. Kirkpatrick. Crystal Growth from the Melt: A Review. Am Mineral. 1975;60:798-814

39. Perepezko, Wilde. Melt Undercooling and Nucleation Kinetics. Curr Opin. Solid State Mater. Sci. 2016;20:3-12

40. Herlach. Non-Equilibrium Solidification of Undercooled Metallic Melts. Metals. 2014;4:196-234

41. Wang. Liquid Supercoolability and Synthesis Kinetics of Quinary Refractory High Entropy. Alloy Sci Rep. 2016.

42. Itami, Okada, Watanabe, Ishikawa, Yoda. Supercooling of Homogeneous Liquid Phase of Liquid Metals and Alloys – Poor Supercooling Around the Eutectic Composition of Liquid Ni-Nb System. Mater Trans. 2010;51:1510-1515

43. Yang. Use of Recalescensce Behaviour Analysis for the Prediction of Grain Refinement in Undercooled Cu-Ni Alloy. J Mater Sci. 2011;46:3101-3107

44. Karma. Model of Grain Refinement in Solidification of Undercooled Melts. Int J Non Equilibr Process. 1998;11:201-233

45. Okamoto, Mueller. Mo (Molybdenum) Binary Alloy Phase Diagrams. 2016.

Citation: E Georgatis, A Poulia, C Mathiou, AE Karantzalis (2022) Solidification Behaviour of Mo$_x$TaNbVTi (x = 0,25 and 0,75) High Entropy Alloys. SOJ Mater Sci Eng 10(1): 1-10.

Page 10 of 10